30. THE VELOCITY STRUCTURE OF LAYER 2 AT DEEP SEA DRILLING PROJECT SITE 504 FROM LOGGING AND LABORATORY EXPERIMENTS[1]

Matthew H. Salisbury, Deep Sea Drilling Project, Scripps Institution of Oceanography
Nikolas I. Christensen, Department of Geosciences, Purdue University
Keir Becker, Deep Sea Drilling Project, Scripps Institution of Oceanography
and
Daniel Moos, Lamont-Doherty Geological Observatory[2]

ABSTRACT

Compressional- and shear-wave velocity logs (V_p and V_s, respectively) that were run to a sub-basement depth of 1013 m (1287.5 m sub-bottom) in Hole 504B suggest the presence of Layer 2A and document the presence of layers 2B and 2C on the Costa Rica Rift. Layer 2A extends from the mudline to 225 m sub-basement and is characterized by compressional-wave velocities of 4.0 km/s or less. Layer 2B extends from 225 to 900 m and may be divided into two intervals: an upper level from 225 to 600 m in which V_p decreases slowly from 5.0 to 4.8 km/s and a lower level from 600 to about 900 m in which V_p increases slowly to 6.0 km/s. In Layer 2C, which was logged for about 100 m to a depth of 1 km, V_p and V_s appear to be constant at 6.0 and 3.2 km/s, respectively. This velocity structure is consistent with, but more detailed than the structure determined by the oblique seismic experiment in the same hole.

Since laboratory measurements of the compressional- and shear-wave velocity of samples from Hole 504B at $P_{confining} = P_{differential}$ average 6.0 and 3.2 km/s respectively, and show only slight increases with depth, we conclude that the velocity structure of Layer 2 is controlled almost entirely by variations in porosity and that the crack porosity of Layer 2C approaches zero. A comparison between the compressional-wave velocities determined by logging and the formation porosities calculated from the results of the large-scale resistivity experiment using Archie's Law suggest that the velocity–porosity relation derived by Hyndman et al. (1984) for laboratory samples serves as an upper bound for V_p, and the noninteractive relation derived by Toksöz et al. (1976) for cracks with an aspect ratio $\alpha = 1/32$ serves as a lower bound.

INTRODUCTION

During the past several decades, our knowledge of the seismic velocity structure of the oceanic crust has improved considerably over the simple three-layer model proposed by Raitt (1963) on the basis of first arrivals. Advances in shooting and recording technology, in particular the development of repetitive sources, sonobuoys, and ocean-bottom seismometers, have led to the recognition of subdivisions in Layers 2 and 3 (Table 1; Sutton et al., 1971; Peterson et al., 1974; Houtz and Ewing, 1976). More recently, the application of inversion techniques and synthetic seismogram analysis to oceanic refraction and reflection data have suggested that the velocity structure of the crust may be more accurately described in terms of velocity gradients (e.g., Helmberger and Morris, 1969; Kennett and Orcutt, 1976; Orcutt et al., 1977; Spudich and Orcutt, 1980).

One of the most striking features of the ocean crust which is emerging from these studies is the variability of Layer 2. Early interpretations of the data by Raitt demonstrated that Layer 2 compressional-wave velocities range widely, from less than 3.0 to more than 6.0 km/s about a mean of 5.07 ± 0.63 km/s (Table 1). More recent interpretations based on sonobuoy data (e.g., Houtz and Ewing, 1976) indicate that Layer 2 may be subdivided into three units: an upper unit (2A) which ranges in velocity from 3 to 4 km/s; an intermediate unit (2B) at greater depth, which ranges between 4.8 and 5.7 km/s, and a lower unit (2C) with a velocity range of 6.0 to 6.4 km/s. Within this context, the variations in Layer 2 ve-

Table 1. Ocean-crust layered velocity models.

Layer	Velocity V_p (km/s)	Thickness (km)
Raitt (1963)		
2	5.07 ± 0.63	1.71 ± 0.75
3	6.69 ± 0.26	4.86 ± 1.42
Mantle	8.13 ± 0.24	—
Peterson et al. (1974)		
1	1.7–2.0	0.5
2A	2.5–3.8	0.5–1.5
2B	4.0–6.0	0.5–1.5
3A	6.5–6.8	2.0–3.0
3B	7.0–7.7	2.0–5.0
Mantle	8.1	—
Houtz and Ewing (1976 Pacific case)		
2A	3.33 ± 0.10	0.74 ± 0.23
2B	5.23 ± 0.44	0.72 ± 0.26
2C	6.19 ± 0.16	1.83 ± 0.75[a]
3	6.92 ± 0.17	—[b]

[a] Cumulative thickness of Layers 2B and 2C.
[b] In general, the mantle and Layer 3B were not detected.

[1] Anderson, R. N., Honnorez, J., Becker, K., et al., *Init. Repts. DSDP*, 83: Washington (U.S. Govt. Printing Office).

[2] Addresses: (Salisbury, present address) Centre for Marine Geology, Dalhousie University, Halifax, Nova Scotia, Canada B3H 3J5; (Becker) Deep Sea Drilling Project A-031, Scripps Institution of Oceanography, University of California at San Diego, La Jolla, CA 92093; (Christensen) Department of Geosciences, Purdue University, West Lafayette, IN 47907; (Moos) Lamont-Doherty Geological Observatory, Palisades, NY 10964.

locity observed by Raitt are interpreted as being due to the presence or absence of one or more of these layers and to regional variations in their thickness. Layer 2A, for example, appears to thin with age (or increase in velocity from below) in the Pacific from about 0.7 km at the ridge crest to 100 m in 30 m.y. old crust, whereas in the Atlantic, it thins from 1.5 km to 100 m over a period of 60 m.y. In both oceans, Layer 2A is generally not detected in older crust, presumably because it is absent or too thin to be detected. Layer 2B, in contrast, is almost always present, but Layer 2C often merges with 2B.

A more sophisticated treatment of the data and one which is consistent with both traveltime and amplitude data suggests that below the uppermost 200 m of basement, which is quite variable, the crust is characterized by a velocity gradient of 0.85 to 1.35/s to a depth of about 2 km. Below this, the crust is relatively homogeneous, with a velocity of about 6.0 km/s which increases more slowly with depth to another steep velocity gradient marking the top of Layer 3 (Whitmarsh, 1978).

With the advent of the Deep Sea Drilling Project, the potential arose for testing these models against the actual velocity structure of the crust as determined by downhole logging. Although several attempts have been made in the past to drill and log deep into the crust (e.g., Kirkpatrick, 1979; Salisbury et al., 1979; Salisbury, 1983; Cann and Von Herzen, 1983), this potential was first fully realized on Leg 83, when Hole 504B on the Costa Rica Rift (Fig. 1) was deepened to a sub-bottom depth of 1350 m and logged to a sub-basement depth of 1013 m through a spectacular sequence of pillow basalts and minor flows underlain by sheeted dikes—a sequence reminiscent of those observed in the upper levels of ophiolites (e.g., Moores and Vine, 1971; Williams, 1971). In addition to conventional logging, high-quality compressional- and shear-wave velocity logs were obtained (the latter for the first time in the ocean crust), using a long-spacing sonic tool (Newmark et al., this volume; Anderson et al., this volume), and estimates of formation porosity were obtained as a function of depth from the results of the large-scale resistivity experiment (Becker, this volume). The purposes of this paper are to present the velocity structure determined for Layer 2 by logging; to compare the results with laboratory measurements of V_p and V_s through samples from Hole 504B held at confining pressures appropriate to the ocean crust; to compare the logging results with the velocity structure determined at the site by means of the oblique seismic experiment (Stephen and Harding, 1983; Little and Stephen, this volume); and, from a comparison with the porosities determined by the large-scale resistivity experiment, to determine the relationship between formation porosity and formation velocity.

DATA

Four data sets are germane to this study: the velocity logs themselves, the rock velocities measured in the laboratory, the formation porosities calculated from the electrical resistivity of the formation, and the refraction velocity structure in the vicinity of the site. Since each of these sets of data is unique in one sense or another, we will outline the means by which they were acquired.

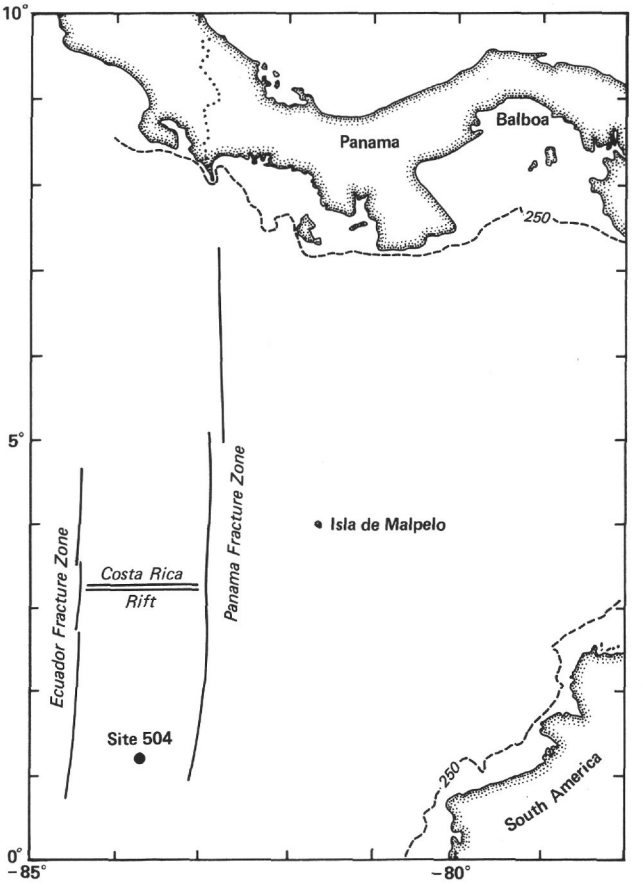

Figure 1. Location of Site 504 on the Costa Rica Rift.

Sonic Velocity Logs

One of the most important data sets, in terms of the seismic velocity structure of the crust, consists of the velocity logs obtained in Hole 504B. These logs, shown in Figure 2, back pocket, were obtained using a Schlumberger long-spacing sonic tool with two 15–32-kHz transmitters and four receivers spaced 8, 10, 10, and 12 ft. from the transmitters. Since this was only the second time the tool had been used in DSDP operations (the first being in several relatively shallow basement holes drilled in the Atlantic on Leg 82; Hill and Cande, in press), the logs shown here represent the longest set of velocity logs obtained in the oceanic crust. More important, several factors contributed to make these logs high in quality: the tool was borehole-compensated and centralized above and below; the long path length between the transmitters and receivers allowed the seismic energy to penetrate fairly deep into the formation, thus bypassing the rugosity of the borehole; and, finally, the borehole had relatively few washouts and was nearly to gauge (10 in.) throughout much of its length (see caliper log in Fig. 2). Although not presented here, repeat logs run with different sondes demonstrate that the logs were reproducible.

In addition to the standard first arrival or P-wave log, an S-wave log was obtained by gating out the P wave and resetting the noise amplitude trigger so that the P-wave softwave picked the S-wave arrival. Although attenuation was relatively minor in the lower levels of the

hole, a decrease in signal amplitude above 655 m, particularly between 15 and 165 m, made it necessary to monitor the signal and occasionally adjust the gain in order to optimize S-wave picking.

In order to evaluate the logs and compare them with the other data sets, interval velocities were calculated for selected intergrated traveltime paths (Fig. 2, back pocket; Table 2). In general, the compressional-wave paths selected were 10 ms long and contiguous, but shorter intervals were sometimes chosen in order to avoid zones of cycle skipping. The shear-wave paths, on the other hand, were selected to coincide with the depth intervals over which the P-wave interval velocities were calculated. Interval velocities were not calculated in washouts, in zones where the logged V_p equalled the fluid velocity, in zones where the logged V_s was less than the fluid velocity, or in zones where the centralizer malfunctioned.

Laboratory Velocity and Porosity Measurements

In order to calibrate the logs and determine the relative influence of alteration and sample porosity on the logging velocities, it is necessary to know the seismic velocities of rock samples from the section logged under conditions of confining pressure and water saturation appropriate to the oceanic crust. To this end, the compressional- and shear-wave velocities of 57 basement samples from Hole 504B were measured in the laboratory at confining pressures of up to 6.0 kbars (Wilkens et al., 1983; Christensen and Salisbury, this volume).

The laboratory velocities presented in Table 2 and back pocket Figure 2 for comparison with the other data sets represent averages of velocities picked or extrapolated to confining pressures equivalent to the differential pressure, P_d, at the depth of recovery of the samples, where:

$$P_{\text{differential}} = P_{\text{lithostatic}} - P_{\text{hydrostatic}}, \quad (1)$$

and $P_{\text{lithostatic}}$ equals the pressure exerted by the water column plus the rock column. Although this pressure is not necessarily appropriate away from the borehole, it would appear to be applicable in the present case since the rocks penetrated by the seismic energy from the sonic logging tool had direct access to seawater at hydrostatic pressure. Support for this assumption is provided by the fact that the velocity logs recorded in several of the massive units in Hole 504B (e.g., between 315 and 330 m sub-bottom and in the sheeted dikes in the bottom of the hole) equal or approach differential, rather than lithostatic-pressure laboratory velocities. Of course this does not prove that the confining pressure equals the differential pressure since even these units could contain fractures.

The wet-bulk densities of the samples were determined from the mass and dimensions of the minicores. After the velocity runs, the minicores were air dried for several weeks and reweighed. The dry-bulk densities were then calculated and the porosities determined from the wet- and dry-bulk densities (Christensen and Salisbury, this volume). In addition to these measurements, a large number of porosity determinations were made on board ship by the same means, but substituting an alternate drying step during which the samples were heated in air for 24 hr. at 110°C in an electric oven prior to the final weighing (Karato et al., 1983). In general, the shipboard measurements gave higher porosities, presumably, because

Table 2. Average basement formation properties from laboratory studies and logging.

Interval (m BSF)	Cores	Lithology	Formation resistivity (Ω-m)	Average sample porosity[a] (%)	*N*	Apparent formation porosity[b] (%)	Fracture porosity[c] (%)	Confining pressure (kbar)	Average sample velocity (km/s)[d] V_p	V_s	*N*	Interval velocity (km/s) V_p	V_s	Interval Poisson's ratio
288–317	4–7		—	5.1	8	—	—	0.02	6.1	3.3	2	4.2	—	—
326–353	9–11		6.3	5.6	6	12.8	7.2	0.02	5.8	3.1	2	—	—	—
362–398	13–17		6.8	5.9	16	12.0	6.1	0.03	6.0	3.2	3	—	—	—
398–439	18–22		8.2	6.1	9	10.7	4.6	0.04	5.9	3.2	3	4.0	—	—
439–480	23–28	Pillow basalts	11.1	5.3	10	9.0	3.7	0.05	5.9	3.2	3	4.2	—	—
480–499	28–30	and	11.7	6.2	4	8.7	2.5	0.05	5.7	3.1	1	5.0	—	—
508–535	32–34	minor flows	14.1	17.9	1	7.8	—	0.06	4.6	2.3	1	5.2	—	—
535–580	35–39		12.2	3.9	6	8.2	4.3	0.07	6.2	3.2	1	5.1	—	—
611–656	44–48		10.6	3.9	6	8.5	4.6	0.08	6.1	3.4	1	4.6	—	—
656–715	49–56		7.2	5.5	8	10.0	4.5	0.09	5.9	3.0	1	5.1	—	—
715–764	57–62		7.0	4.2	7	10.0	5.8	0.10	5.8	3.2	1	5.3	—	—
764–809	63–67		7.1	2.9	5	9.7	6.8	0.11	6.2	3.2	1	4.8	—	—
809–862	68–73		9.8	5.8	7	8.1	2.3	0.12	5.7	3.0	3	4.8	—	—
862–910	74–79		26.7	5.3	4	4.8	−0.5	0.13	5.7	3.0	4	4.8	—	—
910–965	80–85	Transition	57.9	6.5	5	3.2	−3.3	0.14	5.9	3.2	4	5.1	—	—
965–1013	86–91		66.6	3.6	5	3.0	−0.6	0.15	6.1	3.3	4	5.3	—	—
1013–1072	92–98		96.9	2.8	6	2.5	−0.3	0.16	6.2	3.3	3	5.6	—	—
1072–1126	99–104	Sheeted dikes	119.8	2.6	6	2.2	−0.4	0.17	6.2	3.2	3	5.5	—	—
1126–1181	105–114	and	192.2	2.8	7	1.7	−1.1	0.18	6.0	3.2	3	5.9	3.3	0.28
1181–1241	115–124	massive units	222.5	2.4	8	1.6	−0.8	0.19	6.1	3.3	1	6.0	3.2	0.30
1241–1279	125–129		—	1.2	4	—	—	0.20	6.3	3.2	3	6.0	3.2	0.30

Note: Dash indicates that value was not obtained.
[a] Shipboard value.
[b] Calculated from large-scale resistivity data assuming $m = 2.0$.
[c] Formation porosity minus average sample porosity.
[d] At $P_{\text{confining}} = P_{\text{differential}}$.

the higher temperatures used were more effective in driving water from samples. Because these are considered more accurate, only the shipboard porosity measurements are averaged in Table 2 and shown in Figure 2, back pocket.

Oblique Seismic Experiment

In addition to the laboratory and logging data outlined above, the velocity structure of the crust as a whole was determined at Site 504 by means of the oblique seismic experiment. As discussed elsewhere in detail (Stephen et al., 1979; Stephen et al., 1983; Stephen, 1983; Stephen and Harding, 1983; Little and Stephen, this volume), the technique consists of shooting short refraction lines to a borehole seismometer clamped at one or more levels in the basement. Although the resolution of the technique is wavelength-limited, as in conventional refraction studies, the technique is well suited to the purpose of the present study because it provides unusually high resolution in the upper levels of the crust in the immediate vicinity of the site (± 10 km).

During Leg 70, data were recorded in Hole 504B with the seismometer clamped 52 and 542 m into the basement and additional data were recorded by an ocean-bottom seismometer (OBS) array deployed in the vicinity of the site. Although no single velocity–depth profile fits all of the data, the best traveltime model is characterized by a sharp increase in V_p from about 4.2 to 4.8 km/s in the uppermost 200 m of the basement and then by a more gradual increase to 6.0 km/s at a sub-basement depth of 950 m. Below this, V_p increases much more slowly to the top of Layer 3 (6.75 km/s) at a depth of about 2.3 km (Stephen, 1983; Stephen and Harding, 1983). Although the velocity structure at Site 504 is characterized by velocity gradients rather than by homogeneous layers of constant velocity, Stephen (1983) has suggested that the interval from 0–950 m sub-basement represents Layer 2B while the remainder of the section to the top of Layer 3 represents Layer 2C. He also remarks that if the velocity structure were reconstructed from OBS data alone, the velocities of Layers 2B and 2C would be higher, 5.1 and 6.3 km/s, respectively. Velocities consistent with Layer 2A were not detected at the site either by the OBS array or the borehole seismometer.

Large-Scale Resistivity Experiment

In addition to the sample porosities determined in the laboratory, the bulk porosity of the formation was estimated as a function of depth by means of the large-scale resistivity experiment. As discussed by Francis (1981), Becker et al. (1982), and Becker (this volume), this experiment consists of lowering a current electrode and a linear array of potential electrodes down a borehole and monitoring the potential difference between selected electrode pairs as a known DC current passes from the current electrode into the formation and to the ship. Although the technique has lower resolution than conventional resistivity logging, it sees deeper into the formation, past the thermal invasion zone around the borehole, which was cooled by pumping during drilling. Thus the apparent large-scale resistivity, R_a, which is calculated from measured voltages, may give a better value for the true resistivity of the formation at *in situ* temperatures. If, in addition to R_a, the temperature of the formation is known as a function of depth, it is possible to estimate the formation porosity, ϕ, from Archie's Law (1942),

$$\frac{R_a}{R_w} = a\phi^{-m} \tag{2}$$

where R_w is the resistivity of the formation fluid (seawater) and a and m are both constants (see Becker et al., 1982, and Becker, this volume, for a discussion of the many assumptions and qualifications required in applying Archie's Law).

On Leg 83, stationary resistivity measurements were made at 10 m intervals with the potential electrodes spaced 10, 20, 40, and 80 m above the current electrode. To facilitate a direct comparison between the resistivity/porosity data and the logging velocities, only the resistivity data obtained at a 40 m spacing (i.e., between the 40 and 80 m electrodes) will be considered, since this spacing is most nearly equivalent to the average path length for which the interval velocities were determined. The actual resistivity values used in this study (Table 2) were picked near the base of the corresponding velocity interval since the calculated resistivity is considered to be representative of the 40 m interval between the potential electrodes. The formation porosities shown in Table 2 and Figure 2 and referred to later in this paper were then calculated from Archie's Law with a = 1, m = 2.0, and with R_w corrected for the equilibrium formation temperature, which ranges from about 60°C at the sediment/basement contact to about 160°C at the bottom of the hole (Becker et al., 1983; this volume).

DISCUSSION

Data Quality

Prior to interpreting the velocity data obtained by logging at Site 504, it is necessary to establish its validity. Three features of the compressional-wave logs suggest they may be taken at face value: cycle skipping and washouts are rare; the hole is to gauge for more than one third of its length; and the maximum, as opposed to the interval, velocities logged in the massive basalts and dikes in the bottom 125 m of the hole are consistent with laboratory measurements through samples from the same interval (6.0–6.4 km/s; see Fig. 2, back pocket, and Table 2).

Because it is difficult to assess the accuracy of such logs over a range of porosities by visual inspection alone, a more quantitative method of evaluating the logs is needed. As outlined by Tixier (1978), this may be done crudely but effectively for two-phase (rock/water) systems by plotting laboratory velocities versus porosities, as in Figure 3, in order to determine the matrix velocity of the rocks logged (6.4 km/s) and then plotting the sonic log interval transit times (here translated into interval velocities) against formation resistivities on an inverse square root scale as in Figure 4; if the compressional-wave velocities plot on the terminal velocity line defined by the matrix velocity and the fluid resistivity, then the logging values

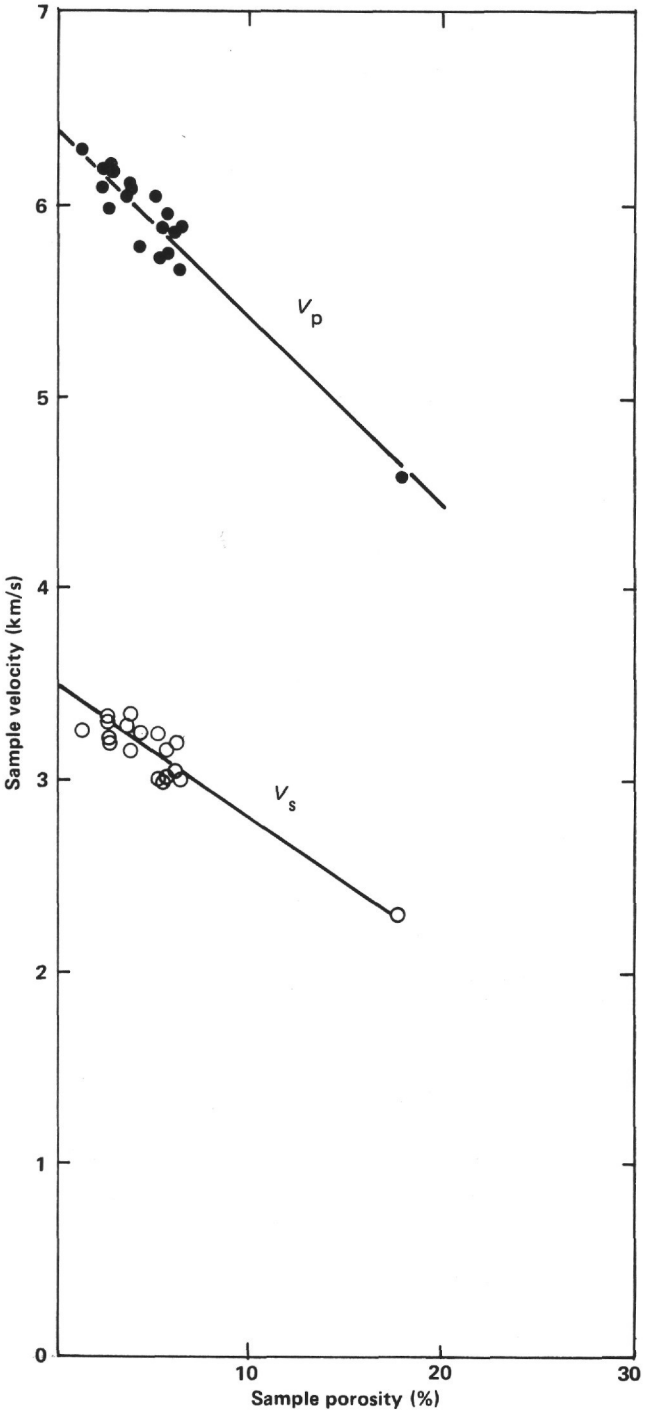

Figure 3. Average laboratory compressional- and shear-wave velocities at elevated pressures ($P_{confining} = P_{differential}$) for rock samples from basement intervals shown in Figure 2 versus average of porosities determined aboard ship for samples for the same intervals. The compressional-wave matrix (zero porosity) velocity is 6.4 km/s.

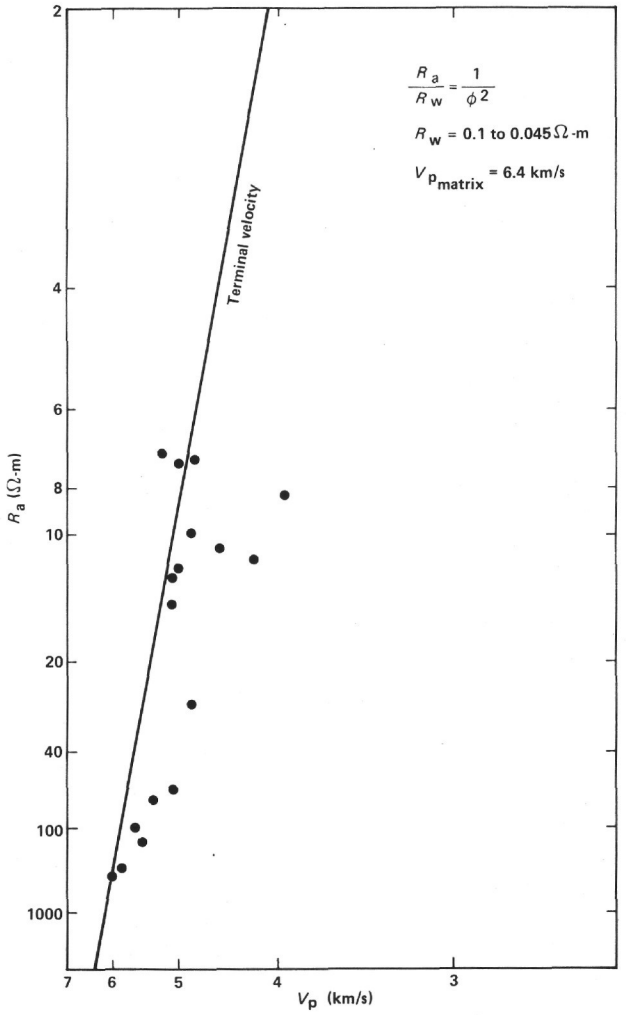

Figure 4. Compressional-wave interval velocities versus formation resistivities determined from the large-scale resistivity experiment. The terminal velocity line is defined by the matrix velocity of basalt (6.4 km/s) and a seawater resistivity of 0.1 to 0.045 Ω-m.

are reasonable. Three assumptions were made in using this approach: (1) that to a first approximation, the transit time varies with porosity and the porosity can be determined from Archie's Law; (2) that only one major rock type, basalt, is present in the hole (Shipboard Scientific Parties, Legs 68, 69, and 70; Hole 504B summary chapter, this volume); and (3) that the formation is saturated with seawater ranging in temperature from 60° to 160°C, which implies that the fluid resistivity, R_w, ranges from 0.1 to 0.045 Ω-m. Strictly speaking, R_w should be constant for this approach to be valid, but the variations in R_w noted here will cause only a small variation in the slope of the terminal velocity line and thus will not affect our conclusions. As will be discussed later, it is not necessary that all velocities plot on the terminal line, but those which do must represent a wide range of formation porosities. This condition is clearly met in Figure 4.

Although the compressional-wave log appears from this test to be valid, the shear-wave data were not shown to be unequivocally valid and were only selectively used in this study. The caliper log run during the shear-wave pass was dead between 75 and 850 m and the shear-wave log for this interval shows little response to changes in lithology (Fig. 2). The only shear-wave data used here were obtained from 0–75 and 850–1000 m when the caliper was working, and even in these intervals the only valid data are from massive units. That the data are valid in these intervals is suggested by the fact that the ve-

locities measured (3.2–3.3 km/s) are consistent with laboratory data (Table 2).

Velocity–Porosity Relations

A glance at Figure 2, back pocket, and Table 2 indicates that the interval velocities obtained for V_p by logging vary considerably in Hole 504B despite the fact that the laboratory velocities of samples from the same intervals show remarkably little variation. V_p, for example, ranges widely from 4.0 to 6.0 km/s whereas the laboratory values, for the most part, range only from 5.7 to 6.3 km/s, about an average of 6.0 km/s. This, together with the uniform composition of the samples recovered from Hole 504B, suggests that the principal control of Layer 2 velocities is not petrology but total formation porosity.

Over the past few decades, several empirical and theoretical attempts have been made to derive a predictive relationship between velocity and formation porosity (Wyllie et al., 1958; O'Connell and Budiansky, 1974; Toksöz et al., 1976). The acquisition of high-quality compressional-wave velocity logs and a more limited set of shear-wave logs in Hole 504B, together with formation porosity data acquired at a comparable scale of investigation, provides the first opportunity to test the applicability of these models to the oceanic crust.

As can be seen in Figure 2, the compressional-wave interval velocity tends to vary with formation porosity. This relationship can be seen more clearly in Figure 5, in which the interval velocities obtained from logging and presented in Table 2 are plotted against the formation porosities derived from the large-scale resistivity experiment. Superimposed on the data are the following: (a) the velocity–porosity relationships derived by Hyndman et al. (1984) from the laboratory velocities reported by Christensen and Salisbury (1975) at elevated pressures,

$$V_p = 6.44 - 9.61\phi + 7.20\phi^2, \quad (3)$$

$$V_s = 3.42 - 6.54\phi + 7.01\phi^2, \quad (4)$$

where ϕ is the porosity expressed as a fraction; (b) the best linear fit to the laboratory data presented here for the samples from Hole 504B at the differential pressure defined above (Christensen and Salisbury, this volume, and Wilkens et al., 1983),

$$V_p = 6.4 - 9.8\phi, \quad (5)$$

$$V_s = 3.5 - 7.0\phi; \quad (6)$$

(c) the relation proposed by Wyllie et al. (1958),

$$\frac{1}{V_p} = \frac{\phi}{V_f} + \frac{(1-\phi)}{V_m} \quad (7)$$

where V_f and V_m are the fluid and matrix velocities, respectively; and (d) solutions to the noninteractive relation of Toksöz et al. (1976) for cracks with aspect ratios, $\alpha = 1/16$ and $1/32$. As can be seen in Figure 5, the relation proposed by Hyndman et al. (1984) provides an upper bound to the data, the noninteractive relation for $\alpha = 1/32$ provides a lower bound, and the solution for $\alpha = 1/16$ provides the best overall fit to the data. Even this relation, however, is far from predictive, since for all but the highest values of V_p, a wide range of porosities is possible.

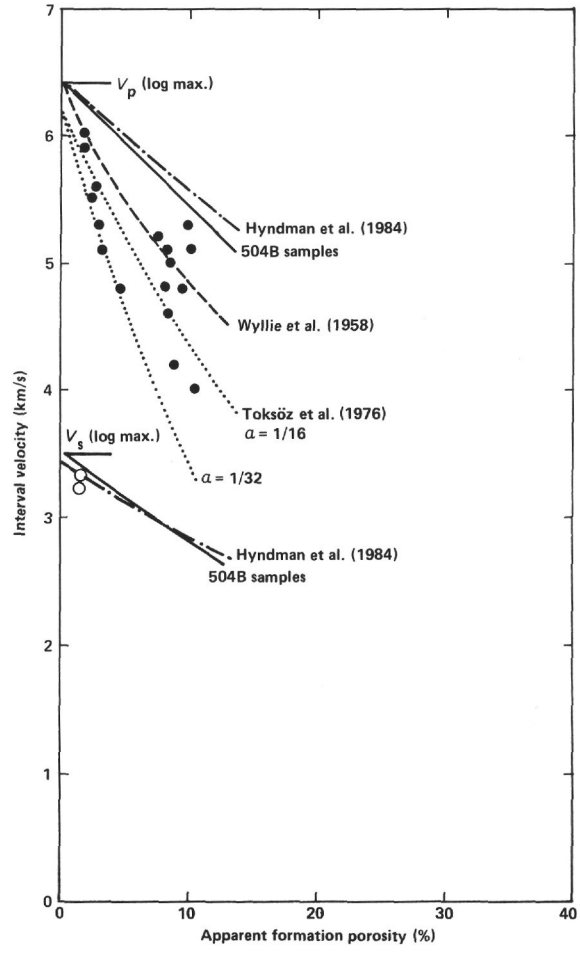

Figure 5. Compressional- and shear-wave interval velocities calculated from logging data versus apparent formation porosities derived from large-scale resistivity data. Superimposed are velocity-porosity relations discussed in the literature and the best fit to the velocities determined in the laboratory for samples from Hole 504B (Wilkens et al., 1983; Christensen and Salisbury, this volume).

Several years ago, a number of authors proposed that the wide range in compressional-wave velocities observed for any given porosity was due to variations in crack configuration (e. g., O'Connell and Budiansky, 1974; Toksöz et al., 1976). Thin cracks, for example, would dramatically decrease V_p, whereas spherical or angular voids and fractures would cause a smaller decrease. This view appears to be confirmed in Figure 6, in which the compressional-wave interval velocities are plotted against estimated fracture porosity (apparent formation porosity minus average sample porosity). Superimposed on this figure are the Hashin–Shtrikman (HS) limits (Hashin and Shtrikman, 1963) with the intersection of the upper and lower bounds set at $V_p = 6.0$ km/s and $\phi = 4.0\%$ (the average velocity and porosity of samples from Hole 504B). As can be seen in this figure, the compressional-wave interval ve-

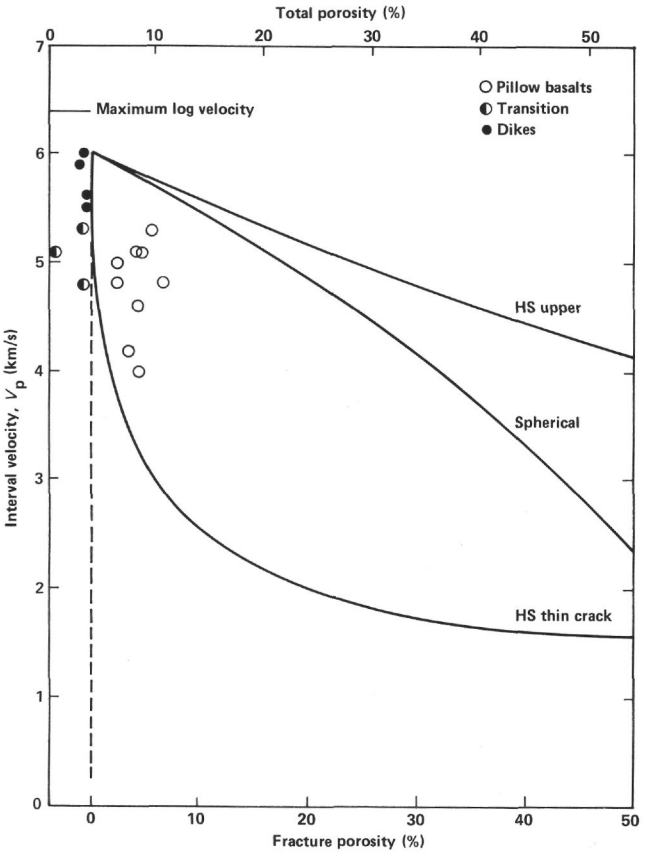

Figure 6. Interval velocity (V_p) versus fracture porosity in Hole 504B. Superimposed are the Hashin–Shtrikman (HS) velocity limits for thin, spherical, and angular voids.

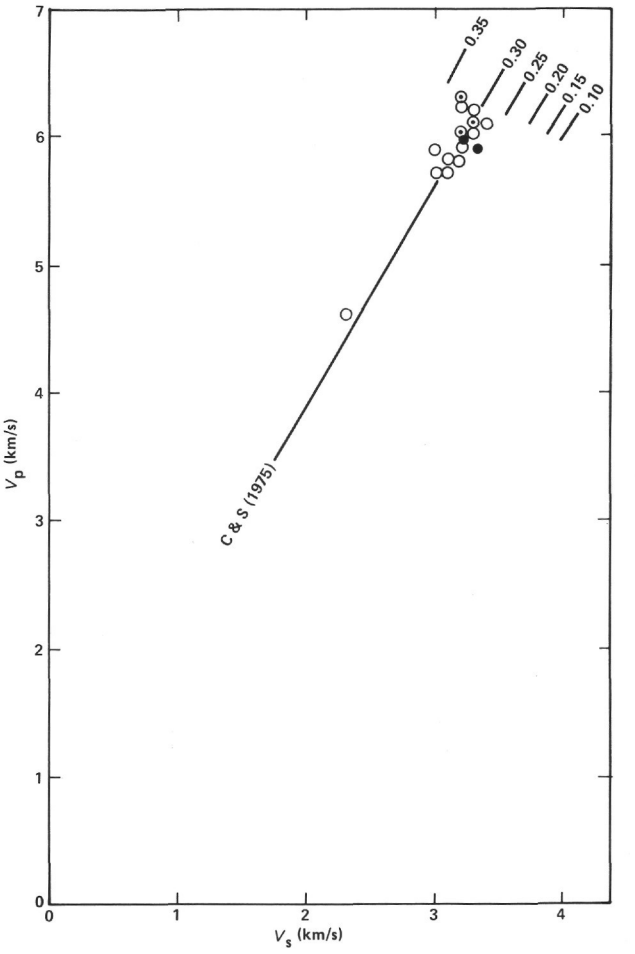

Figure 7. Compressional-wave versus shear-wave interval velocities (solid circles) in Hole 504B. Superimposed are the average velocities determined in the laboratory for samples from the hole (open circles) and a linear solution consistent with the laboratory data presented by Christensen and Salisbury (1975) for DSDP basalts at a confining pressure of 0.5 kbar. The open circles enclosing dots represent laboratory velocities for samples from the sheeted dikes.

locities observed in the sheeted dikes and the overlying transition zone fall on or near the lower or thin-crack HS limit, as would be expected, since the fracture porosity in this unit is almost certainly dominated by joints and thin cracks. The velocities observed in the pillow basalts, on the other hand, range widely between the lower and upper HS bounds, presumably because the void aspect ratio is higher and more variable.

Velocity Versus Poisson's Ratio

Although the velocity in the upper levels of Hole 504B is strongly influenced by formation porosity, the velocities near the base of the hole are controlled largely by petrology. This can be seen clearly in Figure 7 in which the compressional- and shear-wave interval velocities measured in the sheeted dikes approach the velocities measured in the laboratory through samples from the same interval of the hole. Similarly, Poisson's ratio, σ, which is related to V_p and V_s by the relation,

$$\phi = 1/2\left[1 - \frac{1}{(V_p/V_s)^2 - 1}\right] \qquad (8)$$

is seen to range from 0.28 to 0.30 with an average of 0.29, which is slightly less than the sample average of 0.31 in the dikes.

Layer 2 Velocity Structure

Perhaps the most important feature of the logs obtained in Hole 504B is that they represent the first *in situ* determination of the velocity structure of Layer 2. As can be seen in Figure 8, in which the interval velocities and formation porosity are plotted as a function of depth in the hole, V_p increases from about 4.0 to 5.0 km/s in the upper 225 m of the basement. Since V_p is only intermittently observed in this interval, however, we infer that the average velocity of the interval is even lower. Below 225 m, V_p decreases slowly to 4.8 km/s at about 600 m sub-basement, then increases slowly to 6.0 km/s at 900 m and then remains constant to the bottom of the hole. As discussed above, V_s was monitored throughout the hole but the data are considered reliable only below 900 m, where V_s averages 3.2 km/s. On the basis of these data, we conclude that Layers 2A, B and C, as defined by Houtz and Ewing (1976) on the basis of compressional-wave velocity (Table 1), are all present at Site 504: Layer

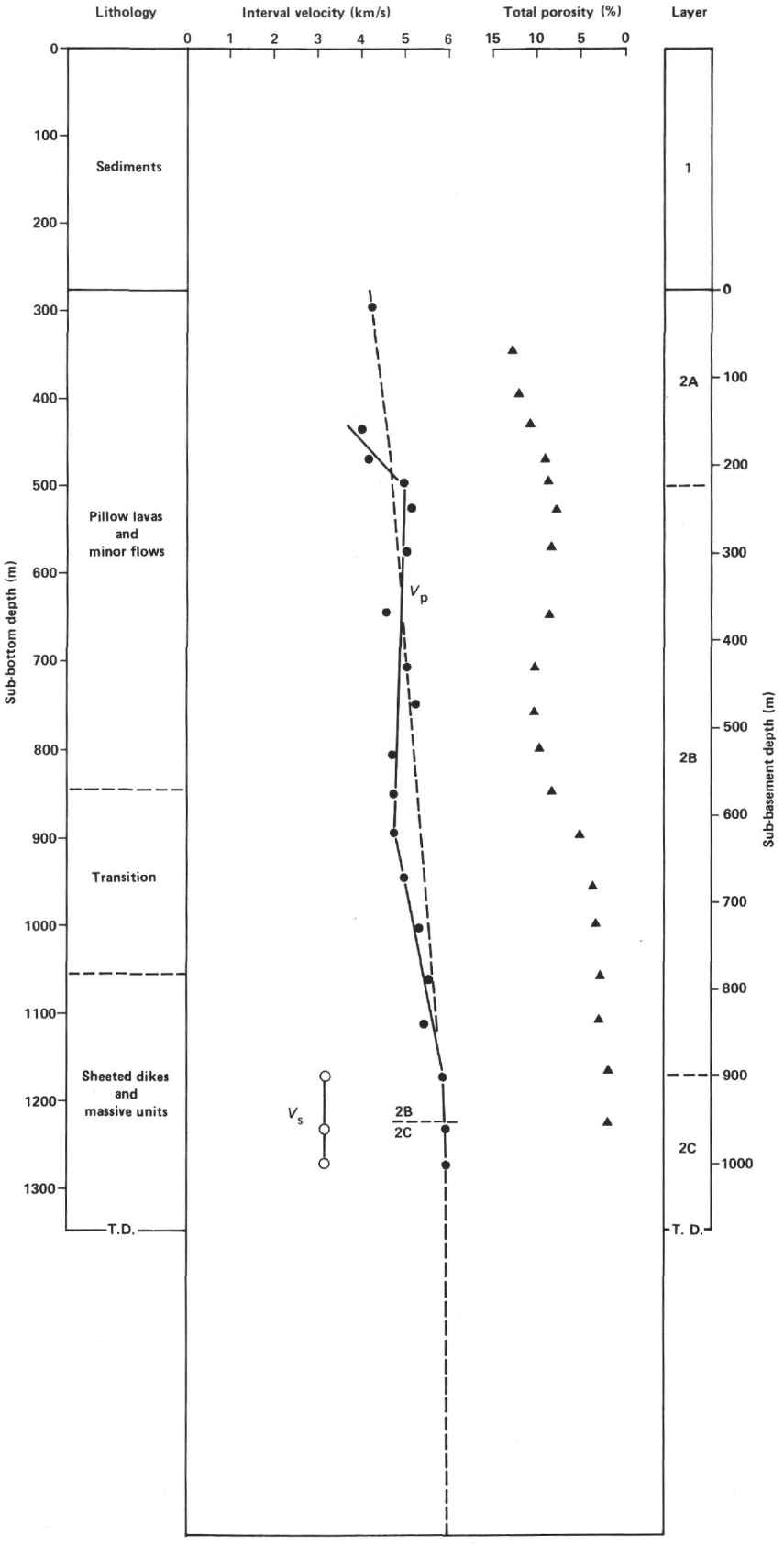

Figure 8. Summary of interval velocities and formation porosity versus depth and lithology in Hole 504B. Also shown are subdivisions defined using the velocity criteria of Houtz and Ewing (1976) for Layers 2A, 2B, and 2C and the velocity structure (dashed line) determined by means of the oblique seismic experiment at Site 504 (Stephen and Harding, 1983).

2A ranges from 0 to 225 m sub-basement; Layer 2B has an average compressional-wave velocity of 5.0 km/s and ranges from 225 to 900 m; Layer 2C ranges from 900 m downward and displays compressional- and shear-wave velocities of 6.0 and 3.2 km/s, respectively (Table 3). It must be emphasized, however, that although the velocity structure at Site 504 can be discussed in terms of Layers 2A, B, and C, it is more accurately described in terms of velocity gradients. In this context, the uppermost layer is characterized by a sharp, but poorly defined positive velocity gradient to a depth of 225 m, where V_p reaches about 5.0 km/s. Below this, V_p decreases at a rate of -0.5/s to 600 m, then increases at a rate of 3.7/s to 900 m, where V_p reaches 6.0 km/s and the gradient goes to zero (Table 3).

Also shown in Figure 8, for comparison with the logging velocity structure, is the velocity structure determined for the site by Stephen and Harding (1983) by means of the oblique seismic experiment. Although the two are basically consistent, it is obvious that logging provides greater detail. The oblique seismic data, for example, suggest the presence of a single, fairly continuous velocity gradient from 0–900 m sub-basement (Layer 2B), whereas the logs indicate the presence of Layer 2A and two subdivisions in 2B within the same interval.

CONCLUSIONS

The recovery of high-quality logs to a depth of 1 km in the basement in Hole 504B on the Costa Rica Rift permits us to reconstruct, for the first time, the velocity structure of Layer 2 from *in situ* data. An examination of these data and a comparison with laboratory velocity studies, refraction data obtained by means of the oblique seismic experiment, and porosity data derived from the large-scale resistivity experiment allow us to reach several major conclusions regarding the nature of Layer 2:

1. As outlined above, Layers 2A, B, and C are all present at Site 504B (Table 3). Layer 2A is approximately 225 m thick, displays a strong velocity gradient (V_p ranges from a maximum of about 4.0 km/s at the top to about 5.0 km/s at the base), and consists of unconsolidated pillow basalts and minor flows. Layer 2B is 675 m thick and consists of two subdivisions, an upper zone which is 375 m thick, in which V_p decreases slowly from 5.0 to 4.8 km/s, and a lower, 300-m thick zone with a positive velocity gradient in which V_p increases from 4.8 to 6.0 km/s. The upper zone consists of pillow basalts and minor flows, whereas the lower zone coincides with the transition zone between the pillow basalts and the underlying sheeted dikes (the dike "screen" zone, in ophiolite terminology). We thus attribute the increase in velocity in the lower half of Layer 2B to the increasing preponderance of massive dikes. Layer 2C, extending from 900 m to at least the bottom of the hole, displays a uniform velocity of 6.0 km/s and consists of relatively unaltered sheeted dikes.

2. Because the samples recovered from Hole 504B have a relatively uniform composition (tholeiitic basalt) and display remarkably uniform velocities (V_p = 6.0 km/s, V_s = 3.2 km/s), we conclude, as have others (e.g., Whitmarsh, 1978; Spudich and Orcutt, 1980), that porosity is the principal factor controlling velocity in the levels penetrated to date. Comparisons between compressional-wave interval velocities and formation and fracture porosities confirm this relationship and indicate that the noninteractive solution of Toksöz et al. (1976) for α = 1/16 represents a poor, but nonetheless the best overall fit to the data, with the laboratory data providing an upper bound and the noninteractive solution for α = 1/32 providing the lower bound. Within this context, the compressional-wave velocity structure in Layer 2A is due to a decrease in apparent formation porosity from 13% at the top of the unit to 9% at the base, whereas the velocity structure of Layer 2B is controlled by a small increase in porosity to about 10% at intermediate levels, followed by a steady decrease to about 2% (i.e., zero fracture porosity) at the top of Layer 2C.

3. The scatter in the velocity–porosity data, particularly for V_p, is due to variations in the percentage and configuration of cracks. In formations with low fracture porosity ($\leq$1%), V_p may be depressed by as much as 1 km/s by the presence of even a small number of cracks. Thus we feel Layer 2C is virtually sealed at Site 504. In formations such as pillow basalts with a higher fracture porosity ($\sim$10%), and a range of crack aspect ratios, V_p may be depressed even more. Thus the problem of determining porosity from refraction data may not always be tractable. Where the fracture porosity is low, however, as

Table 3. Layer 2 velocity structure at Site 504.

Homogeneous layer model												
Layer	Depth[a] (m)	V_p (km/s)	V_s (km/s)	ϕ[b] (%)	Depth[a] (m)	V_p[c] (km/s)	$\frac{dV_p}{d_z}$ (s^{-1})	V_s[c] (k/ms)	$\frac{dV_s}{d_z}$ (s^{-1})	ϕ[c] (%)	$\frac{d\phi}{d_z}$[b] (%/km)
2A	0				0	—		—		13	
		—	—	11.1			—		—		−18
	225				225	5.0		—		9	
							−0.5		—		−11
2B		5.1	—	6.7	600	4.8		—		5	
							+3.7		—		−10
	900				900	5.9		3.2		2	
2C		6.0	3.2	1.7			0		0		0

[a] Meters sub-basement.
[b] Formation porosity.
[c] At top of layer.

in Layer 2C and deeper, the data presented here suggest that the petrology of the formation may be determined at depth using the V_p/V_s technique described by Christensen and Salisbury (1975) and refined by Spudich and Orcutt (1980).

4. Finally, it should be remarked that whereas a great deal of refraction data has been gathered for the oceanic crust over the past several decades, using a variety of techniques ranging from simple surface refraction shooting to borehole seismometer studies, there has been no way until now to confirm or deny its validity. At Site 504, OBS studies detected Layers 2B and 2C but tended to read high in velocity (or deeper on the velocity gradient) and missed Layer 2A entirely (Stephen, 1983). The oblique seismic experiment, in contrast, obtained data which are basically consistent with the *in situ* logging data, but missed Layer 2A and the velocity increase at the base of 2B corresponding to the screen zone (Stephen and Harding, 1983). Although such discrepancies may never be entirely reconciled (they could, for example, be due to lateral heterogeneity), it is clear that refraction data are rapidly approaching *in situ* data in quality.

ACKNOWLEDGMENTS

We wish to express our appreciation to the captain, crew, and technical staff to the *Glomar Challenger* on Leg 83 for their assistance during the deployment of the large-scale resistivity experiment, to Frank Foster of Schlumberger Ltd. for his assistance in running the long-spacing sonic tool and to Barry Goldman for his assistance in obtaining the laboratory velocity measurements. The laboratory measurements were supported by ONR contract N-00014-80-C-0252 and the resistivity measurements were conducted under NSF Grant OCE-81-17693.

REFERENCES

Archie, G. E., 1942. The electrical resistivity log as an aid in determining some reservoir characteristics. *J. Petrol. Tech.*, 5:1–8.

Becker, K., Langseth, M. G., Von Herzen, R. P., and Anderson, R. N., 1983. Deep crustal geothermal measurements, Hole 504B, Costa Rica Rift. *J. Geophys. Res.* 88:3447–3457.

Becker, K., Von Herzen, R. P., Francis, T. J. G., Anderson, R. N., Honnorez, J., Adamson, A. C., Alt, J. C., Emmermann, R., Kempton, P. D., Kinoshita, H., Laverne, C., Mottl, M. J., and Newmark, R. L., 1982. *In situ* electrical resistivity and bulk porosity of the oceanic crust Costa Rica Rift. *Nature*, 300:594–598.

Birch, F., 1960. The velocity of compressional waves in rocks to 10 kbar, 1. *J. Geophys. Res.*, 65:1083–1102.

_____, 1961. The velocity of compressional waves in rocks to 10 kbar, 2. *J. Geophys. Res.*, 66:2199–2224.

Cann, J. R., Von Herzen, R. P., 1983. Downhole logging at Deep Sea Drilling Project Sites 501, 504, and 505, near the Costa Rica Rift. *In* Cann, J. R., Langseth, M. G., Honnorez, J., Von Herzen, R. P., White, S. M., et al., *Init. Repts. DSDP*, 69: Washington (U.S. Govt. Printing Office), 281–299.

Christensen, N. I., and Salisbury, M. H., 1975. Structure and constitution of the lower oceanic crust. *Rev. Geophys. Space Phys.*, 13: 57–86.

Francis, T. J. G., 1981. Large-scale resistivity experiment at Deep Sea Drilling Project Hole 459B. *In* Hussong, D. M., Uyeda, S., et al., *Init. Repts. DSDP*, 60: Washington (U.S. Govt. Printing Office), 841–852.

Hashin, Z., and Shtrikman, S., 1963. A variational approach to the theory of the elastic behavior of multiphase materials. *J. Mech. Phys. Solids*, 2:127–140.

Helmberger, D. V., and Morris, G. B., 1969. A travel time and amplitude interpretation of a marine refraction profile: primary waves. *J. Geophys. Res.*, 74:483–494.

Hill, I. A., and Cande, S. C., in press. Downhole logging and laboratory physical property measurements on DSDP Leg 82. *In* Bougault, H., Cande, S. C., et al., *Init. Repts. DSDP*, 82: Washington (U.S. Govt. Printing Office).

Houtz, R., and Ewing, J., 1976. Upper crustal structure as a function of plate age. *J. Geophys. Res.*, 81:2490–2498.

Hyndman, R. D., Christensen, N. I., and Drury, M. J., 1984. The physical properties of basalt core samples from Deep Sea Drilling Project Leg 78B Hole 395A. *In* Hyndman, R. D., Salisbury, M. H., et al., *Init. Repts. DSDP*, 78B: Washington (U.S. Govt. Printing Office), 801–810.

Karato, S., Wilkens, R. H., and Langseth, M. G., 1983. Shipboard physical-properties measurements of basalts from the Costa Rica Rift, Deep Sea Drilling Project, Legs 69 and 70. *In* Cann, J. R., Langseth, M. G., Honnorez, J., Von Herzen, R. P., White, S. M., et al., *Init. Repts. DSDP*, 69: Washington (U.S. Govt. Printing Office), 675–695.

Kennett, B. N. L., and Orcutt, J. A., 1976. A comparison of travel time inversions for marine refraction profiles. *J. Geophys. Res.*, 81:4061–4070.

Kirkpatrick, R. J., 1979. The physical state of the oceanic crust: Results of downhole geophysical logging in the Mid-Atlantic Ridge at 23° N. *J. Geophys. Res.*, 84:178–188.

Moores, E. M., and Vine, F. J., 1971. The Troodos massif, Cyprus, and other ophiolites as oceanic crust: Evaluation and implications. *Phil. Trans. R. Soc. London, Ser. A*, 268:443–466.

O'Connell, R. J., and Budiansky, B., 1974. Seismic velocities in dry and saturated cracked solids. *J. Geophys. Res.*, 79:5412–5426.

Orcutt, J. A., Dorman, L. M., and Spudich, P. K. P., 1977. Inversion of seismic refraction data. *In* Heacock, J. G., (Ed.), *The Earth's Crust*. Am. Geophys. Un., Geophys. Monogr. Ser., 20:371–384.

Peterson, J. J., Fox, P. J., and Schreiber, E., 1974. Newfoundland ophiolites and the geology of the oceanic layer. *Nature*, 247: 194–196.

Raitt, R. W., 1963. The crustal rocks. *In* Hill, M. N. (Ed.), *The Sea* (Vol. 3), 85–102: New York (John Wiley).

Salisbury, M. H., 1983. Basement logs from the mouth of the Gulf of California. Deep Sea Drilling Project Leg 65. *In* Lewis, B. T. R., Robinson, P., et al., *Init. Repts. DSDP*, 65: Washington (U.S. Govt. Printing Office), 329–342.

Salisbury, M. H., Donnelly, T. W., and Francheteau, J., 1979. Geophysical logging in Deep Sea Drilling Project Hole 417D. *In* Donnelly, T., Francheteau, J., Bryan, W., Robinson, P., Flower, M., Salisbury, M., et al., *Init. Repts. DSDP*, 51, 52, 53, Pt 1: Washington (U.S. Govt. Printing Office), 705–713.

Shipboard Scientific Parties of Leg 68 (Site 501), Leg 69, and Leg 70, 1983. Sites 501 and 504: Sediments and ocean crust in an area of high heat flow on the southern flank of the Costa Rica Rift. *In* Cann, J. R., Langseth, M. G., Honnorez, J., Von Herzen, R. P., White, S. M., et al., *Init. Repts. DSDP*, 69: Washington (U.S. Govt. Printing Office), 31–173.

Spudich, P., and Orcutt, J. A., 1980. Petrology and porosity of an oceanic crust site: Results from waveform modeling of seismic refraction data. *J. Geophys. Res.*, 85:1409–1433.

Stephen, R. A., 1983. The oblique seismic experiment on Deep Sea Drilling Project Leg 70. *In* Cann, J. R., Langseth, M. G., Honnorez, J., Von Herzen, R. P., White, S. M., et al., *Init. Repts. DSDP*, 69: Washington (U.S. Govt. Printing Office), 301–308.

Stephen, R. A., and Harding, A. J., 1983. Travel time analysis of borehole seismic data. *J. Geophys. Res.*, 88:8289–8298.

Stephen, R. A., Johnson, S., and Lewis, B. T. R., 1983. The oblique seismic experiment on DSDP Leg 65. *In* Lewis, B. T. R., Robinson, P., et al., *Init. Repts. DSDP*, 65: Washington (U.S. Govt. Printing Office), 319–327.

Stephen, R. A., Louden, K. E., and Matthews, D. H., 1979. The oblique seismic experiment on DSDP Leg 52. *In* Donnelly, T., Francheteau, J., Bryan, W., Robinson, P., Flower, M., Salisbury, M., et al., *Init. Repts. DSDP*, 51, 52, 53, Pt. 1: Washington (U.S. Govt. Printing Office), 675–704.

Sutton, G. H., Maynard, G. L., and Hussong, D. M., 1971. Widespread occurrence of a high-velocity basal layer in the Pacific crust found with repetitive sources and sonobouys. *In* Heacock, J. G. (Ed.), *The Structure and Physical Properties of the Earth's Crust*. Am. Geophys. Un., Geophys. Monogr. Ser., 14:193–209.

Tixier, M. P., 1978. Quality control and procedure for processing logs of Legs 46, 48, 50, 51, 57, 60, 61 [unpublished report].

Toksöz, N., Cheng, C. H., and Timur, A., 1976. Velocities of seismic waves in porous rocks. *Geophysics*, 41:621–645.

Whitmarsh, R. B., 1978. Seismic refraction studies of the upper igneous crust in the North Atlantic and porosity estimates for Layer 2. *Earth Planet. Sci. Lett.* 37:451–464.

Wilkens, R. H., Christensen, N. I., and Slater, L., 1983. High pressure seismic studies of Leg 69 and 70 basalts. *In* Cann, J. R., Langseth, M. G., Honnorez, J., Von Herzen, R. P., White, S. M., et al., *Init. Repts. DSDP*, 69: Washington (U.S. Govt. Printing Office), 683–686.

Williams, H., 1971. Mafic-ultramafic complexes in western Newfoundland Appalachians and the evidence for transportation: a review and interim report. *Proc. Geol. Ass. Can.*, 24(1):9–25.

Wyllie, M. R. J., Gregory, A. R., and Gardner, G. H. F., 1958. An experimental investigation of factors affecting elastic wave velocities in porous media. *Geophysics* 23:459–493.

Date of Initial Receipt: 31 January 1984
Date of Acceptance: 29 August 1984